ISBN: 978-3-95450-231-8 ISSN: 2673-5490 doi: 10.18429/JACoW-IPAC2023-TUPL190

PHASE SPACE MEASUREMENTS OF AN ELECTRON BEAM USING THE ASU CRYOCOOLED 200 kV DC ELECTRON GUN

G. S. Gevorkyan*, C. A. Sarabia-Cardenas†, P. Bhattacharyya, M. M. Rizi, S. Karkare‡
Arizona State University, Tempe, AZ, USA

Abstract

The cryocooled DC electron gun at Arizona State University is the first electron gun built to implement single-crystal, ordered surface and epitaxially grown photocathodes to produce cold and dense electron beams at the source. These high brightness electron sources are extremely desirable for ultrafast electron applications such as Xray Free Electron Lasers, Ultrafast Electron Diffraction/Microscopy, and electron-ion colliders. Electron beams are produced from a cryogenically cooled photocathode using a tunable wavelength laser to emit electrons close to the photoemission threshold. The full four-dimensional transverse phase space of the electron beam can be measured by a Pinhole Scan technique, allowing us to directly calculate the transverse emittance in both dimensions. In this contribution we report and discuss the beamline setup for the 4D transverse phase space measurement and first results.

INTRODUCTION

Major upgrades to electron beam dependent time resolved tools such as X-ray Free Electron Lasers (XFEL), Ultrafast Electron Diffraction (UED), Ultrafast Electron Microscopy (UEM), and linear electron colliders for fundamental physics research can be realized with brighter electron beams created by novel photocathodes [1]. XFELs in particular will benefit from improvements to the brightness of electron beams at the source as this produces higher pulse energies and photon lasing energies [2] and enables them to be built in a compact framework suitable for university laboratories which will increase their reach in STEM research [3]. At this time, there is a push to improve the normalized transverse emittance which is critical to UED/M and directly related to electron beam brightness [4–7]. The measure of brightness for photoemission-based linear electron accelerators, or photoinjectors, with low longitudinal and transverse coupling [1] is the 4D beam brightness, which can be given by:

$$B_{4D} \propto \frac{E_0^n}{\mathrm{MTE}}, \tag{1}$$

where E_0 is the accelerating electric field at the photocathode surface at the time of electron emission, and n is a number between 1 and 2 depending on the aspect ratio of the electron beam [8, 9]. MTE is the mean transverse energy, equal to $\frac{1}{2}m_0\langle v_\perp^2\rangle$ where m_0 is the electron rest mass and $v_\perp$ is the electron velocity in the direction transverse to the beam propagation. MTE is related to the normalized RMS emittance as:

$$\epsilon_{ni} = \sigma_i\sqrt{\mathrm{MTE}/m_0c^2}, \tag{2}$$

where ϵ_{ni} is the emittance in a direction transverse to the beam propagation, σ_i is the RMS transverse size of the electron beam, and m_0c^2 is the rest mass energy of the electron. There are active efforts to improve brightness by creating higher electric fields; this has been successful through the use of RF guns [10], but further improvements require a reduction in emittance. MTE is limited by a number of factors, namely things like the choice of the photocathode, the photocathode's lattice temperature, the cathode surface quality, and the wavelength of light used for electron emission.

A low MTE is primarily limited by a high excess energy, E_{ex}, which is the difference between the photon energy and the photocathode work function [11]:

$$\mathrm{MTE} \approx E_{\mathrm{ex}}/3. \tag{3}$$

This can be resolved by using electrons that are emitted from the tail of the Fermi distribution in metals, which is done by tuning the photon energy to the work function such that the excess energy is zero or slightly negative. This results in MTE being limited instead by the photocathode lattice temperature as:

$$\mathrm{MTE} \approx k_BT, \tag{4}$$

where T is the cathode temperature and k_B is the familiar Boltzmann constant [12]. Modern photoinjectors fall into a range of MTE of a few 100 meV [13–16] due to their choice of laser and cathode. Recent works have suggested using single-crystalline, atomically ordered photocathodes as next generation bright electron sources [17–21], and in particular epitaxially grown alkali-antimonides [22, 23].

A cryogenically cooled 200 kV DC electron gun and accompanying photocathode diagnostics beamline has been commissioned at ASU [4, 24] with an objective to test such novel materials as cathodes. This electron gun has a versatile photocathode mounting capability, a cryogenic cooling capability, the necessary surface preparation tools, and a tunable wavelength laser for photoemission. In this paper, we describe the beamline connected to this gun for 4D transverse phase space measurements.

PINHOLE SCAN TECHNIQUE FOR FULL 4D PHASE SPACE MEASUREMENTS

In Fig. 1, we show the current accelerator beamline with various elements highlighted for clarity. The beamline consists of 8 corrector dipole magnets to steer the electron beam, two solenoid magnets for transverse focusing, an aperture

* Ggevorky@asu.edu
† Casarab1@asu.edu
‡ Karkare@asu.edu

ISBN: 978-3-95450-231-8 ISSN: 2673-5490 doi: 10.18429/JACoW-IPAC2023-TUPL190

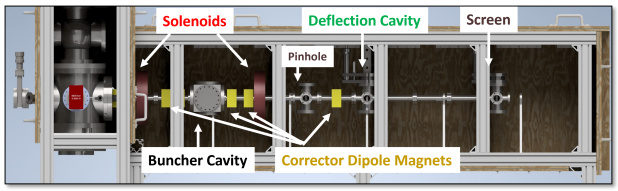

Figure 1: The beamline consists of corrector dipole magnets (yellow), two solenoid magnets (red), a 3.0 GHz buncher cavity, a "pinhole" aperture element, a 3.0 GHz deflection cavity, and multiple YAG screens.

element, a 3.0 GHz buncher cavity of the Eindhoven design [25] for longitudinal focusing, and a 3.0 GHz deflection cavity. The final element is a YAG:Ce scintillator screen coupled to a CMOS camera and lens. In this beamline we plan to implement a solenoid scan emittance measurement [26], a time response measurement [26], a beam cropping phase space measurement [27, 28], and eventually UED in the stroboscopic and single-shot modes [29–31].

The emittance in Eq. (2) is a critically important measurement of an electron beam in relation to the beam brightness in Eq. (1). To find emittance, we use a Pinhole Scan technique to measure the full 4D phase space using an aperture element to select a section of the focused electron beam and illuminate a detector screen after some drift space. This technique was developed at the MEDUSA beamline in Cornell University [5, 28, 32]. An illustration of the technique is shown in Fig. 2.

In our beamline we use a thin tantalum foil with 10 µm, 30 µm, and 80 µm apertures to crop to a small portion of the focused electron beam. After the beam is cropped, the electrons pass through a drift space before they reach the scintillator screen which allows us to measure the transverse momentum spread. The phase space measured will give us enough information to calculate the 4D beam matrix, which is the two RMS transverse positions and momenta and their related correlations

$$\Sigma_{4D} = \begin{bmatrix} \langle xx \rangle & \langle xx' \rangle & \langle xy \rangle & \langle xy' \rangle \\ \langle x'x \rangle & \langle x'x' \rangle & \langle x'y \rangle & \langle x'y' \rangle \\ \langle yx \rangle & \langle yx' \rangle & \langle yy \rangle & \langle yy' \rangle \\ \langle y'x \rangle & \langle y'x' \rangle & \langle y'y \rangle & \langle y'y' \rangle \end{bmatrix}. \quad (5)$$

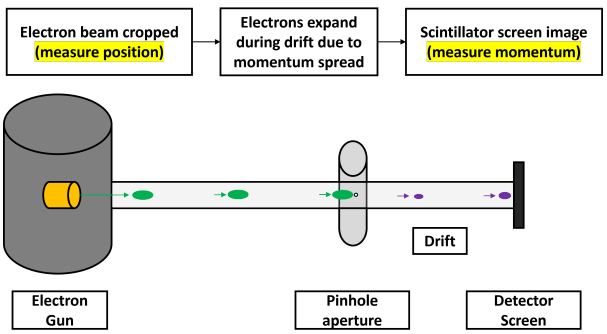

Figure 2: This is an illustration of the Pinhole Scan technique. Beam position is measured at the aperture, and the momentum spread is measured after a drift space.

In the equation, x and y represent the transverse position of the beam at the aperture, and the primed coordinates are derivatives with respect to longitudinal position and represent the transverse momentum. We use this matrix to calculate the 4D normalized emittance and determine the mean transverse energy (MTE) of the beam

$$\epsilon_{4D,n} = (\gamma\beta)^2\sqrt{\det(\Sigma_{4D})}, \quad (6)$$

where det is the determinant of the matrix. The 4D emittance can then be used to find the electron beam MTE,

$$\text{MTE} = \frac{\epsilon_{4D,n}}{\sigma_i^2 m_0 c^2}. \quad (7)$$

In this equation, σ_i is the RMS laser spot size and m_0c^2 is the rest mass energy of a free electron.

IMPLEMENTING THE PINHOLE SCAN AT THE ASU CRYOGUN BEAMLINE

Simulations of Phase Space Measurements

We modeled this Pinhole Scan technique in GPT [33] and analyzed the results in MATLAB. We simulated our expected beam parameters and real beamline elements to compute an image comparable to our real detector screen and CMOS camera. The beam was rastered over the aperture by adjusting the simulated corrector coils. We then used MATLAB to compute the full 4D phase space of the beam using the resulting images of the simulation. Using simulation, have predicted results for a large range of values for MTE's and beam spot sizes we expect to measure.

The smallest emittance that can be measured is limited by the aperture used, the resolution of the screen and camera system, and the distance between the aperture and the screen. In our setup the drift distance is 0.7 m. For this drift a 1.0 µm spot on the screen corresponds to a transverse momentum of 0.30 eV/c. Assuming a 50 µm resolution of the YAG screen and the camera-lens imaging system, we get a precision of of 14.97 eV/c in the measured σ_{px}. If we use the 10 µm aperture, the smallest possible emittance that can be measured is 0.53 nm-rad.

Measurements on the Beamline

In Fig. 3, we show a Pinhole Scan of a beam from a Cs_3Sb photocathode on a molybdenum substrate. This photocathode was significantly degraded since it had been in the electron gun for over two months since growth. A 532 nm continuous laser with 5 mW power was focused to the center 100 µm of the photocathode. A flip mirror was used to direct the laser beam to a intensity profiler matching the distance to the photocathode to measure the laser spot size, which was measured to be 70 µm RMS. The beam was focused and centered onto the 80 µm aperture. We rastered the beam in small steps using an advanced optimized scanning strategy to suppress errors due to systematic drift [34, 35]. Each image was 811-by-811 pixels and the resolution was 13.636 µm per pixel. Our MATLAB code interpreted these

ISBN: 978-3-95450-231-8 ISSN: 2673-5490 doi: 10.18429/JACoW-IPAC2023-TUPL190

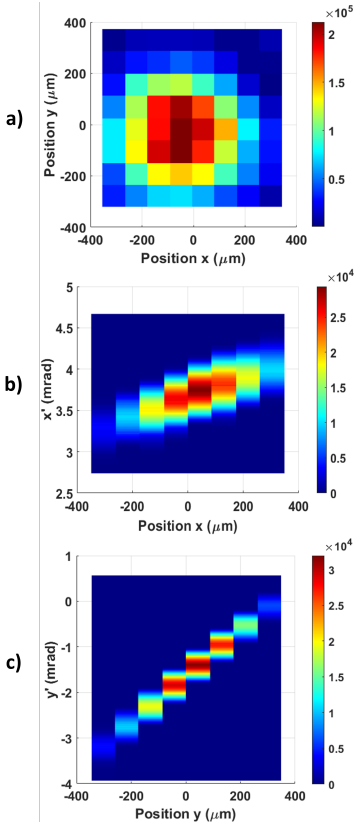

Figure 3: A full 4D phase space was reconstructed from our degraded Cs_3Sb photocathode grown on molybdenum using the Pinhole Scan technique. This was measured in our beamline at 30 keV with a spot size of 70 µm. We show the transverse positions x-y (a), where σ_x = 158.53 µm and σ_y = 151.02 µm. In (b) and (c), we plot the 2D phase space in one transverse axes x-x' and y-y' respectively, $\sqrt{\epsilon_{4D}}$ = 27.1 nm-rad.

images to compute the matrix is Eq. (5) and emittance in Eq. (6). Using Eq. (7), we measured an MTE of 76.6 meV for our degraded Cs_3Sb sample using 532 nm light.

CONCLUSION

Future automation of this code can be implemented to remove as much of the manual operation of the beam as possible, particularly in the dipole coil momentum calibration and in the actual measurement process. Testing single-crystalline cathodes at cryogenic temperatures will be a priority because they have demonstrated record low transverse energy spreads, and measuring the full 4D phase space of such materials at high voltage in optimal conditions is currently only possible using this electron gun and beamline.

Cryogenic cooling was not used because the laser was significantly above threshold energy for Cs_3Sb. The next iteration of this beamline will use our tunable wavelength laser, which has a 500 kHz repetition rate and a FWHM pulse length of 150 fs from a pulsed Optical Parametric Amplifier. We expect to see a difference in the emittance after tuning the wavelength to threshold and cryogenically cooling the photocathode [17]. This beamline will eventually be used for UED in both the stroboscopic and single-shot modes [31, 36, 37], making it possible to surpass the k-space resolution of existing UED tools, given proper beam quality preservation, due to the ability to make use of higher brightness sources in our electron gun.

ACKNOWLEDGEMENTS

The authors would like to thank Charles Zhang, Chad Pennington, and their advisor Dr. Jared Maxson for their help in this project. This work was supported by the U.S. National Science Foundation under Award No. PHY-1549132, the Center for Bright Beams, and the DOE under Grant No. DE-SC0021092.

REFERENCES

[1] P. Musumeci *et al.*, "Advances in bright electron sources," *Nucl. Instrum. Methods Phys. Res., Sect. A*, vol. 907, pp. 209–220, 2018. doi:10.1016/j.nima.2018.03.019

[2] X. Wang *et al.*, "Report of the basic energy sciences workshop on the future of electron sources," *DOE Technical Report*, 2016. doi:10.2172/1616511

[3] J. B. Rosenzweig *et al.*, "An ultra-compact x-ray free-electron laser," *New J. Phys.*, vol. 22, no. 9, p. 093 067, 2020. doi:10.1088/1367-2630/abb16c

[4] G. S. Gevorkyan *et al.*, "Design of a 200 kV DC cryocooled photoemission gun for photocathode investigations," in *Proc. NAPAC'22*, Albuquerque, NM, USA, 2022, pp. 292–295. doi:10.18429/JACoW-NAPAC2022-TUYD6

[5] W. H. Li *et al.*, "A kiloelectron-volt ultrafast electron microdiffraction apparatus using low emittance semiconductor photocathodes," *Struct. Dyn.*, vol. 9, no. 2, p. 024 302, 2022. doi:10.1063/4.0000138

[6] N. Stoffel and P. Johnson, "A low-energy high-brightness electron gun for inverse photoemission," *Nucl. Instrum. Methods Phys. Res., Sect. A*, vol. 234, no. 2, pp. 230–234, 1985. doi:10.1016/0168-9002(85)90910-6

[7] C. Hernandez-Garcia *et al.*, "High voltage studies of inverted-geometry ceramic insulators for a 350 kV DC polarized electron gun," *IEEE Trans. Dielectr. Electr. Insul.*, vol. 23, no. 1, pp. 418–427, 2016. doi:10.1109/TDEI.2015.005126

[8] A. Arnold and J. Teichert, "Overview on superconducting photoinjectors," *Phys. Rev. ST Accel. Beams*, vol. 14, p. 024 801, 2011. doi:10.1103/PhysRevSTAB.14.024801

[9] D. H. Dowell and J. F. Schmerge, "Quantum efficiency and thermal emittance of metal photocathodes," *Phys. Rev. ST Accel. Beams*, vol. 12, p. 074 201, 2009. doi:10.1103/PhysRevSTAB.12.074201

[10] T. Vecchione *et al.*, "Quantum Efficiency and Transverse Momentum From Metals," pp. 424–426, https://jacow.org/FEL2013/papers/TUPSO83.pdf

[11] J. Feng *et al.*, "Thermal limit to the intrinsic emittance from metal photocathodes," *Appl. Phys. Lett.*, vol. 107, no. 13, p. 134 101, 2015. doi:10.1063/1.4931976

ISBN: 978-3-95450-231-8 ISSN: 2673-5490 doi: 10.18429/JACoW-IPAC2023-TUPL190

[12] G. S. Gevorkyan *et al.*, "Effects of physical and chemical surface roughness on the brightness of electron beams from photocathodes," *Phys. Rev. Accel. Beams*, vol. 21, p. 093 401, 2018. doi:10.1103/PhysRevAccelBeams.21.093401

[13] P. Saha *et al.*, "Physically and chemically smooth cesium-antimonide photocathodes on single crystal strontium titanate substrates," *Appl. Phys. Lett.*, vol. 120, no. 19, p. 194 102, 2022. doi:10.1063/5.0088306

[14] C. T. Parzyck *et al.*, "Single-crystal alkali antimonide photocathodes: High efficiency in the ultrathin limit," *Phys. Rev. Lett.*, vol. 128, p. 114 801, 2022. doi:10.1103/PhysRevLett.128.114801

[15] F. Sannibale *et al.*, "APEX Phase-II commissioning results at the Lawrence Berkeley National Laboratory," in *Proc. IPAC'16*, Busan, Korea, 2016, pp. 1041–1043. doi:10.18429/JACoW-IPAC2016-TUOCA02

[16] J. Rosenzweig *et al.*, "Ultra-high brightness electron beams from very-high field cryogenic radiofrequency photocathode sources," *Nucl. Instrum. Methods Phys. Res., Sect. A*, vol. 909, pp. 224–228, 2018, 3rd European Advanced Accelerator Concepts workshop (EAAC2017). doi:10.1016/j.nima.2018.01.061

[17] S. Karkare *et al.*, "Reduction of intrinsic electron emittance from photocathodes using ordered crystalline surfaces," *Phys. Rev. Lett.*, vol. 118, p. 164 802, 2017. doi:10.1103/PhysRevLett.118.164802

[18] J. K. Nangoi *et al.*, "Importance of bulk excitations and coherent electron-photon-phonon scattering in photoemission from PbTe(111): Ab initio theory with experimental comparisons," *Phys. Rev. B*, vol. 104, p. 115 132, 2021. doi:10.1103/PhysRevB.104.115132

[19] C. J. Knill *et al.*, "Near-Threshold Nonlinear Photoemission From Cu(100)," in *Proc. IPAC'21*, Campinas, Brazil, May 2021, pp. 2822–2825. doi:10.18429/JACoW-IPAC2021-WEPAB099

[20] S. Karkare *et al.*, "Ultracold electrons via near-threshold photoemission from single-crystal Cu(100)," *Phys. Rev. Lett.*, vol. 125, p. 054 801, 2020. doi:10.1103/PhysRevLett.125.054801

[21] L. Cultrera *et al.*, "Cold electron beams from cryocooled, alkali antimonide photocathodes," *Phys. Rev. ST Accel. Beams*, vol. 18, p. 113 401, 2015. doi:10.1103/PhysRevSTAB.18.113401

[22] D. Alesini *et al.*, "New technology based on clamping for high gradient radio frequency photogun," *Phys. Rev. ST Accel. Beams*, vol. 18, p. 092 001, 2015. doi:10.1103/PhysRevSTAB.18.092001

[23] P. A. Adderley *et al.*, "Load-locked dc high voltage gaas photogun with an inverted-geometry ceramic insulator," *Phys. Rev. ST Accel. Beams*, vol. 13, p. 010 101, 2010. doi:10.1103/PhysRevSTAB.13.010101

[24] G. S. Gevorkyan *et al.*, "Design of a 200 kV DC cryocooled photoemission gun for photocathode investigations," in *Proc. NAPAC'19*, Lansing, MI, USA, 2019, pp. 136–139. doi:10.18429/JACoW-NAPAC2019-MOPLM16

[25] T. van Oudheusden, "Electron source for sub-relativistic single-shot femtosecond diffraction," Ph.D. dissertation, Applied Physics, 2010. doi:10.6100/IR693519

[26] I. V. Bazarov *et al.*, "Thermal emittance and response time measurements of negative electron affinity photocathodes," *J. Appl. Phys.*, vol. 103, no. 5, p. 054 901, 2008. doi:10.1063/1.2838209

[27] F. Ji *et al.*, "Knife-edge based measurement of the 4D transverse phase space of electron beams with picometer-scale emittance," *Phys. Rev. Accel. Beams*, vol. 22, p. 082 801, 2019. doi:10.1103/PhysRevAccelBeams.22.082801

[28] M. Gordon *et al.*, "Four-dimensional emittance measurements of ultrafast electron diffraction optics corrected up to sextupole order," *Phys. Rev. Accel. Beams*, vol. 25, p. 084 001, 2022. doi:10.1103/PhysRevAccelBeams.25.084001

[29] C.-Y. Ruan *et al.*, "Ultrafast diffraction and structural dynamics: The nature of complex molecules far from equilibrium," *Proc. Natl. Acad. Sci. U.S.A.*, vol. 98, no. 13, pp. 7117–7122, 2001. doi:10.1073/pnas.131192898

[30] A. H. Zewail, "4D ultrafast electron diffraction, crystallography, and microscopy," *Annu. Rev. Phys. Chem.*, vol. 57, pp. 65–103, 2006. doi:10.1146/annurev.physchem.57.032905.104748

[31] T. Van Oudheusden *et al.*, "Compression of subrelativistic space-charge-dominated electron bunches for single-shot femtosecond electron diffraction," *Phys. Rev. Lett.*, vol. 105, no. 26, p. 264 801, 2010. doi:10.1103/PhysRevLett.105.264801

[32] C. J. R. Duncan *et al.*, "Multi-scale time-resolved electron diffraction enabled by high repetition rate, high dynamic range direct electron detection," *arXiv*, 2022. doi:10.48550/arXiv.2206.08404

[33] S. B. van der Geer and M. J. de Loos, "Applications of the General Particle Tracer Code," in *Proc. PAC'97*, Vancouver, Canada, May 1997, pp. 2577–2579.

[34] V. V. Yashchuk, "Optimal measurement strategies for effective suppression of drift errors," *Rev. Sci. Inst.*, vol. 80, no. 11, p. 115 101, 2009. doi:10.1063/1.3249559

[35] I. Lacey *et al.*, "Development of a high performance surface slope measuring system for two-dimensional mapping of x-ray optics," in *Adv. Metrol. X-Ray EUV Opt. VII*, SPIE, vol. 10385, 2017, pp. 103–115. doi:10.1117/12.2273029

[36] T. van Oudheusden *et al.*, "Electron source concept for single-shot sub-100 fs electron diffraction in the 100 keV range," *J. Appl. Phys.*, vol. 102, no. 9, p. 093 501, 2007. doi:10.1063/1.2801027

[37] R. Li *et al.*, "Note: Single-shot continuously time-resolved mev ultrafast electron diffraction," *Rev. Sci. Inst.*, vol. 81, no. 3, p. 036 110, 2010. doi:10.1063/1.3361196